Combustion of Methanol and Methanol/Dodecanol Spray Flames

C. Presser, A. K. Gupta, C. T. Avedisian, H. G. Semerjian

Reprinted from

Journal of Propulsion and Power

Volume 8, Number 3, May–June 1992, Pages 553–559

AIAA

A publication of the
American Institute of Aeronautics and Astronautics, Inc.
The Aerospace Center, 370 L'Enfant Promenade, SW
Washington, DC 20024-2518

JOURNAL OF PROPULSION AND POWER
Vol. 8, No. 3, May–June 1992

Combustion of Methanol and Methanol/Dodecanol Spray Flames

C. Presser*
National Institute of Standards and Technology, Gaithersburg, Maryland 20899
A. K. Gupta†
University of Maryland, College Park, Maryland 20742
C. T. Avedisian‡
Cornell University, Ithaca, New York 14853
and
H. G. Semerjian§
National Institute of Standards and Technology, Gaithersburg, Maryland 20899

The structure of methanol and methanol/dodecanol mixture spray flames has been examined. The mixture was studied in order to obtain evidence for the occurrence of microexplosions. Droplet size and velocity measurements were carried out under burning conditions using phase/Doppler interferometry. Laser sheet beam photography was used to observe the global features of the spray within the nonluminous portion of the flames. Droplet size and velocity distributions near the nozzle exit were found to be similar and monomodal for both fuels. Further downstream in the mixture flame, the velocity distribution became bimodal near the spray boundary along with a change in size distribution to smaller droplets and an increase in number density. These results suggest that microexplosions occur in 50/50 mixtures of methanol/dodecanol spray flames.

I. Introduction

ALCOHOL fuels are becoming increasingly important because of their potential as a replacement for conventional fossil fuels (i.e., gasoline, heating oils, etc.) in various power and propulsion systems.[1] They are generally nonsooting, particularly the more volatile alcohols, and burn more cleanly as nonluminous blue flames. Data obtained from alcohol fuels also facilitate comparison of experiments with relevant theories of spray performance. Practical fuels are seldom single component. Binary mixtures are the simplest mixtures that can be used to examine the effect of fuel composition. A study of mixtures also offers the possibility of examining the phenomenon of microexplosions. Finally, a study of burning sprays is relevant to such applications as gas turbine combustors, automotive engines, spray-fired waste incinerators, and industrial furnaces.

Results are presented on the structure of spray flames, fueled by methanol and a 50/50 mixture by volume of methanol and 1-dodecanol. The equivolume mixture was selected because it has been used in studies of burning single droplets.[2,3] Droplet size and velocity distributions were obtained using a phase/Doppler interferometry system.[4,5] Laser sheet beam photography was also used to observe the global features of pressure-atomized spray flames.

II. Experimental Arrangement

Experiments were carried out in a spray combustion facility that was designed to simulate practical combustion systems. The facility includes a swirl burner with a moveable 12-vane swirl cascade; the vanes are rotated simultaneously to impart the desired degree of swirl intensity to the coflowing combustion air stream. The spray facility permits examination of the effects of combustion air swirl, atomizer design, fuel properties, equivalence ratio, and air preheat on spray structure and combustion characteristics. The swirl strength introduced to the combustion air is given in terms of the swirl number S, which is determined according to the theory outlined in Ref. 6. Experiments were carried out for $S = 0.53$ under burning conditions.

A simplex pressure-jet nozzle is located along the centerline of the burner. The fuel nozzle was operated at total air and fuel flow rates of 64.3 kg/h and 3.2 kg/h, respectively. The spray is injected vertically upward from the nozzle, which is located at the burner exit. The pressure-jet nozzle provides a nominal 60-deg hollow-cone spray. A stepper-motor-driven

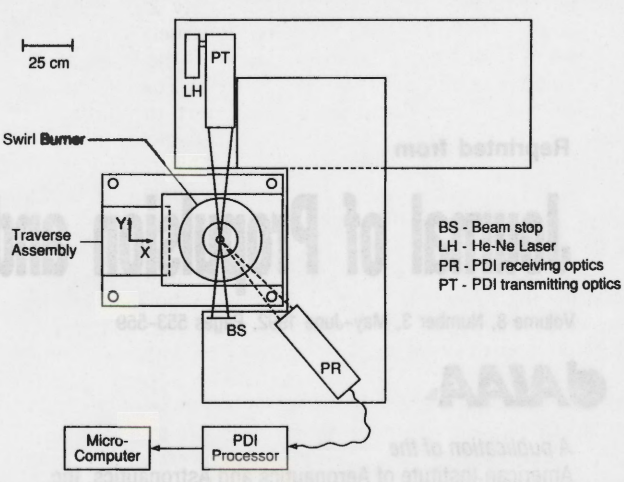

Fig. 1 Schematic of experimental droplet size/velocity facility.

Presented as Paper 90-2446 at the AIAA/SAE/ASME/ASEE 26th Joint Propulsion Conference, Orlando, FL, July 16–18, 1990; received Nov. 19, 1990; revision received April 29, 1991; accepted for publication May 7, 1991.

*Research Engineer, High Temperature Processes Group, Chemical Science and Technology Laboratory. Associate Fellow AIAA.

†Professor, Department of Mechanical Engineering. Fellow AIAA.

‡Associate Professor, Sibley School of Mechanical & Aerospace Engineering. Member AIAA.

§Chief, Process Measurements Division, Chemical Science and Technology Laboratory. Member AIAA.

three-dimensional traversing arrangement is used to translate the burner assembly in the vertical (Z) and both horizontal (X and Y) directions. All optical diagnostics are fixed in position about the burner assembly so that the burner can translate independently of the optical equipment. This arrangement permits precise alignment of the measurement volume within the spray (see Fig. 1). Measurement of radial profiles of the spray flame properties, e.g., droplet size and velocity distributions, can then be carried out at different axial positions. Further details on the experimental arrangement are given elsewhere.[7]

Droplet size and velocity distributions were measured using a single-channel phase/Doppler interferometer. Measurements are carried out as particles pass through the probe volume defined by the intersection of two laser beams. This intersection of laser beams creates an interference fringe pattern. A modulated signature (Doppler burst) is detected as a particle passes through the probe volume and scatters light. A receiving lens is located at an off-axis collection angle and projects a portion of this fringe pattern onto three detectors. Each detector produces a Doppler signal with a frequency proportional to particle velocity. The phase shift between the Doppler signals from the different detectors is proportional to the size of spherical particles. The instrument provides in-situ, nonintrusive information at different positions within the spray. For these experiments, an off-axis light collection system was used, with the optics positioned at a scattering angle of 30 deg. The focal length of the transmitting and receiving optics was 495 and 500 mm, respectively. A 10-mW He-Ne laser, operating at a wavelength of 632.8 nm, provided the light source. The signal data rate was kept at a relatively low value (approximately 200 Hz) by adjusting the supply voltage for the scattered light detector. A total of 5000 data points were recorded for each measurement. The repeatability was generally better than 5% near the nominal spray boundary.

Interpretation of the experimental measurements is facilitated by acquiring an initial qualitative understanding of the complex flow patterns associated with the spray flame. To this end, an argon ion laser sheet beam of about 1 mm thickness, was used to examine various horizontal and vertical cross sections (through the centerline) of the spray flame. The relative position of the fuel spray within the flame envelope was recorded with a 35-mm camera; the exposure times varied from $\frac{1}{4}$ to $\frac{1}{60}$ s.

III. Results and Discussion

A. Global Features of the Spray Flame

The luminosity of spray flames produced by methanol and methanol/dodecanol was observed to be different. Figure 2 reveals that the methanol flame forms a relatively nonluminous plume. By contrast, the methanol/dodecanol mixture formed a hybrid flame that was characterized by a nonluminous blue zone (extending to approximately Z = 75 mm), followed by a luminous zone. This hybrid structure may have its origin in the preferential vaporization of the mixture due to the relative volatility of the components. For example, in diffusion-controlled liquid-phase transport methanol will dominate vaporization initially (with the flame color corresponding to that of a methanol flame). This region will be followed by dodecanol vaporization with a concomitant change in the color of the flame; hence, the hybrid nature of the flame (see Ref. 3).

In the blue, nonluminous portions of each flame, laser sheet beam photography was used to illuminate the detailed features of the fuel spray under burning conditions. Therefore, the relative position of the fuel spray cone within the flame plume can be observed if the flame remains optically transparent. For example, Fig. 3 shows the structure of the methanol spray flame using laser sheet beam photography to illuminate the fuel droplets. The larger droplets are generally observed along the spray boundary and remain relatively unperturbed by the surrounding aerodynamic pattern, which controls the structure of the flame envelope. Many of these droplets penetrate through the flame sheet relatively unburned and into the surrounding environment at downstream positions ($Z \approx 100$ mm). The methanol/dodecanol flame also revealed similar features in the nonluminous portion of the flame. Further downstream ($Z > 75$ mm) illumination of the droplets within the plume by the laser sheet was difficult because of the high background flame radiation. In this case, laser sheet beam photography can only be used to observe droplets that penetrate through the flame plume into the surrounding environment.

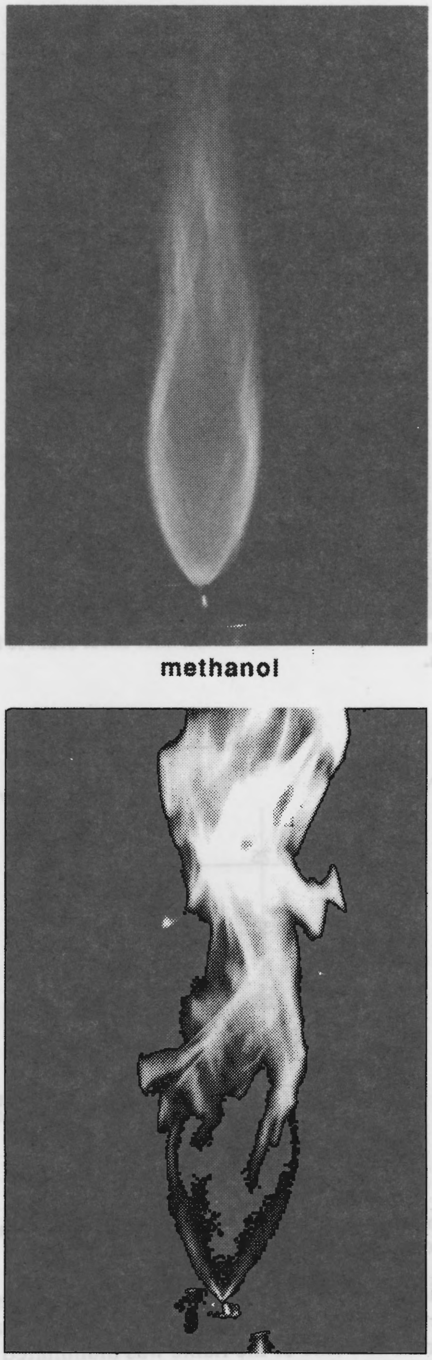

Fig. 2 View of the methanol and methanol/dodecanol flames.

A horizontal laser sheet beam was also used to illuminate the droplets that were found outside the flame sheet of both flames. It was observed for $Z > 76.2$ mm that the flame resided on the inside surface of the spray, whereas at upstream positions the flame sheet surrounded the spray (see Fig. 3).

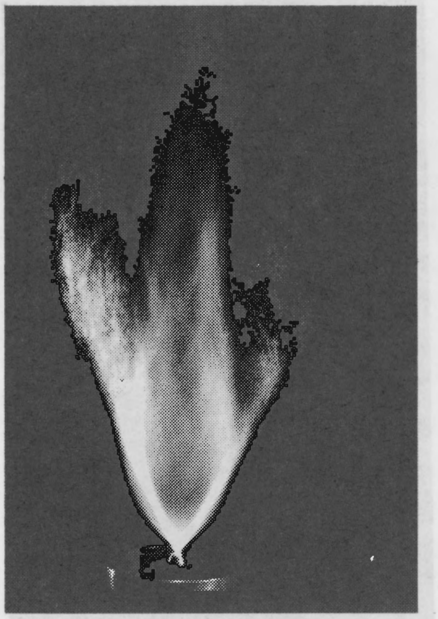

Fig. 3 **View of the methanol flame with laser sheet beam to illuminate fuel droplets.**

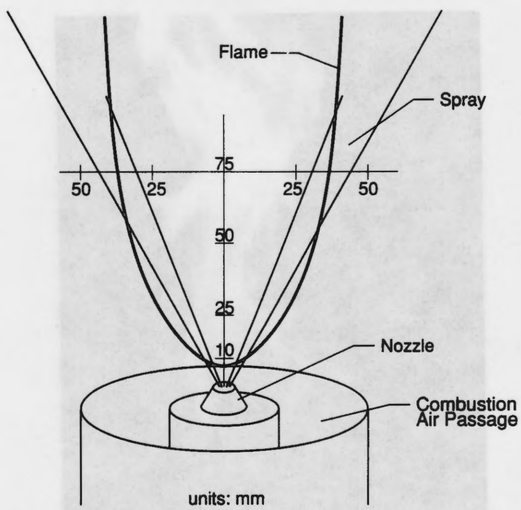

Fig. 4 Schematic of the flames indicating position of the spray boundary relative to the flame sheet.

A schematic of the position of the spray boundary relative to the flame envelope is shown in Fig. 4. For the methanol and mixture flames one side of the flame was illuminated in order to observe the droplets outside of the flame sheet at $Z = 76.2$ mm (see Fig. 5). Several droplets outside the flame were observed to develop long streaks for the mixture flame (see arrow in Fig. 5); no such streaks were observed in the methanol flame. These long streaks may result from microexplosions of the methanol/dodecanol droplets in the spray flame. When a microexplosion occurred, the droplet formed a relatively long streak when photographed; these streaks were random in length and direction, and did not align with the flow direction. The width of these droplet streaks were observed to be larger than the neighboring droplets. This may be attributed to the diffusion flame burning of these smaller droplets and the subsequent luminous emission from the flamelets. To explore further the possibility of the occurrence of microexplosions in the methanol/dodecanol flame quantitative data on droplet size, velocity and number density were recorded using phase/Doppler interferometry.

B. Droplet Mean Diameter, Velocity and Number Density

The phase/Doppler interferometry system was used to obtain spatially resolved information on the droplets under burn-

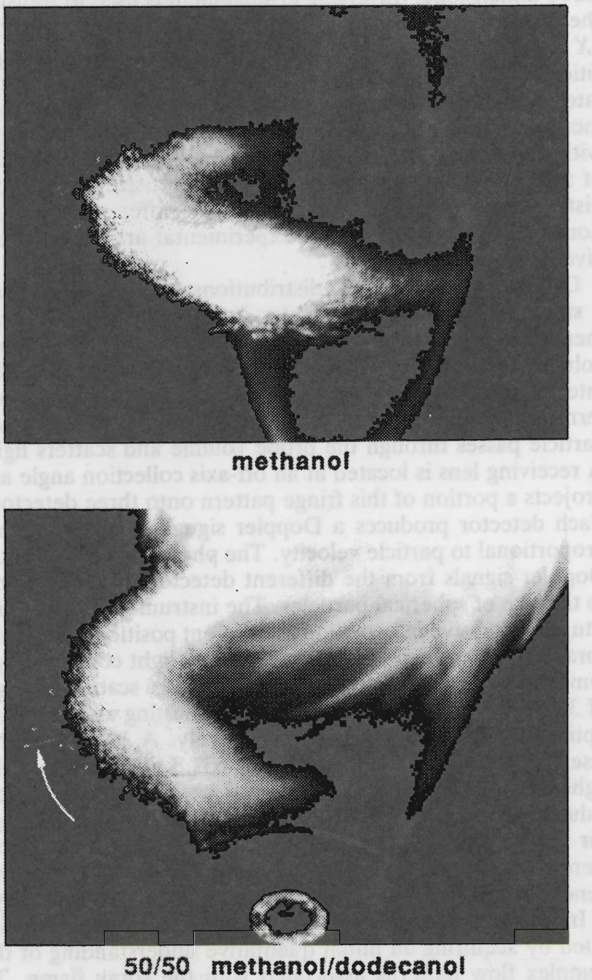

Fig. 5 View of the methanol and methanol/dodecanol flames with laser sheet beam to illuminate fuel droplets at $Z = 76.2$ mm. Droplet streaks indicate possible evidence of microexplosions (see arrow).

ing conditions. The values of Sauter mean diameter (D_{32}) are presented in Fig. 6 for methanol and methanol/dodecanol mixture at $Z = 10$, 25.4, 50.8, and 76.2 mm. The solid boxes along the abscissa indicate the position of the burner passage walls, with the fuel nozzle located at the centerline. The vertical lines that intersect each profile represent positions of the observed outer boundary of the spray flame. The position of these lines was estimated from the observed position of the flame sheet in Fig. 3 and the falloff in total validated counts from the phase/Doppler measurements. Limited data are presented at $Z = 50.8$ and 76.2 mm because of the very low data rate in the central region of the spray flame. The variation of D_{32} with spatial position is typical of hollow-cone pressure-atomized spray flames. The droplets near the spray boundary (defined by the peaks in the D_{32} distributions) are larger than those near the spray centerline in the upstream portion of the spray. The profiles become more uniform with increasing axial position.

Comparison of these data for both fuels indicates that droplet mean diameter for the methanol/dodecanol flame is larger than the methanol flame near the centerline and outside the flame sheet at $Z \leq 25.4$ mm (see Fig. 6). At these positions preferential vaporization of the smaller droplets will result in larger values of D_{32} for the methanol/dodecanol flame. This behavior can be attributed to the higher volatility of methanol relative to dodecanol (the boiling point of methanol is 338 K as compared to 529 K for dodecanol).

In the region between the outer spray boundary and flame sheet, the droplet mean size of the methanol/dodecanol mixture is larger than that of methanol at $Z = 10$ mm. At pro-

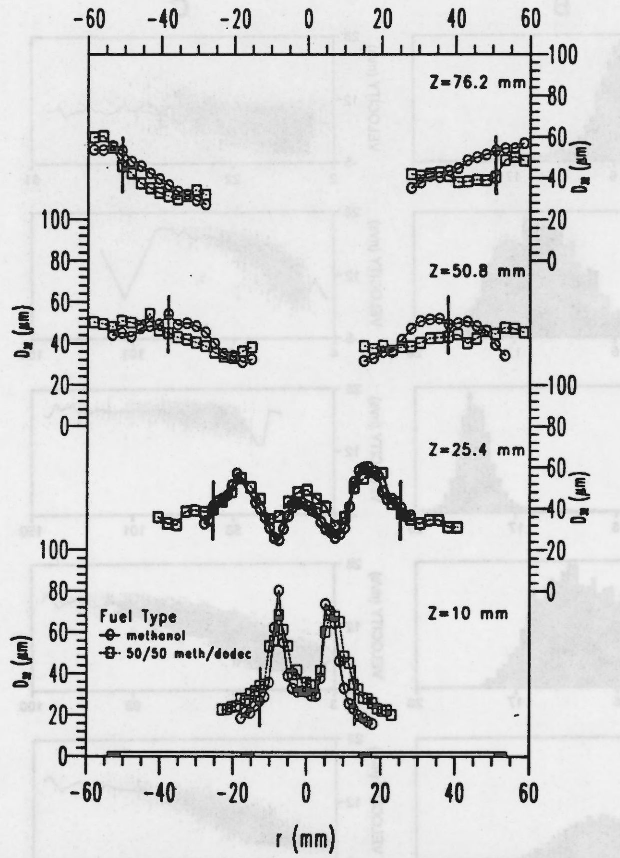

Fig. 6 Variation of droplet Sauter mean diameter (D_{32}) with radial position (r) at different axial positions (Z) for the methanol and methanol/dodecanol flames. Vertical lines indicate outer boundary of the spray flame.

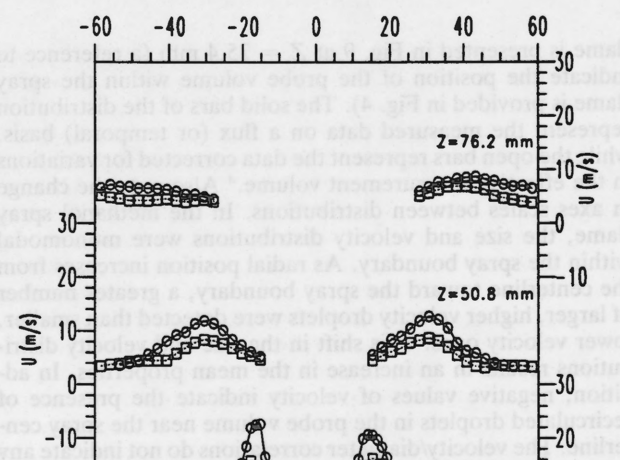

Fig. 7 Variation of droplet mean axial velocity (U) with radial position (r) at different axial positions (Z) for the methanol and methanol/dodecanol flames.

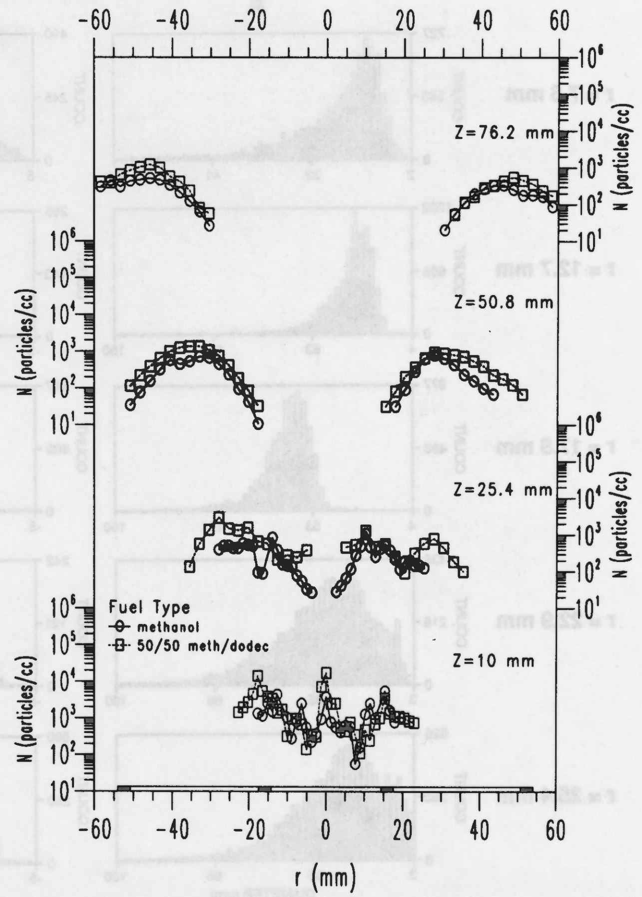

Fig. 8 Variation of droplet number density (N) with radial position (r) at different axial positions (Z) for the methanol and methanol/dodecanol flames.

gressive axial positions the droplet mean diameter of the mixture becomes smaller than that of methanol. This suggests that the mixture droplets may have microexploded. In addition, it is noted that near the spray boundary the profiles of D_{32} are similar for both fuels in the upstream portion of the spray ($Z \leq 25.4$ mm).

Radial profiles of droplet mean axial velocity (U) for the methanol and mixture flames are shown in Fig. 7 at $Z = 10$, 25.4, 50.8, and 76.2 mm. The mean velocity profiles are also indicative of the overall characteristics of hollow-cone spray flames; namely, the highest velocities are found near the spray boundary. The variation of velocity between the two fuels is most prominent near the spray boundary where the values of U for the methanol/dodecanol flame are lower than for methanol. This trend is to be expected, because the droplet size and velocity would be inversely proportional for a given initial droplet momentum. These findings are in agreement with the results found in the literature.[8]

C. Observations Related to Microexplosions

Microexplosion of droplets produces several smaller droplets from a single larger droplet. This would result in a sudden decrease in the value of D_{32} for the mixture relative to methanol with increasing axial position. In addition, microexplosions may yield a difference between number density of the mixture and methanol. Droplet velocity would be expected to increase initially because of the energy imparted to the droplets, and then dissipate when these smaller droplets are entrained into the surrounding flow field. Figure 6 shows that at $Z = 50.8$ and 76.2 mm, in the region between the outer spray boundary and flame sheet, the values of D_{32} for the mixture are substantially smaller than for methanol. Figure 8 shows that the number density for the mixture is larger than that of methanol in this region (cf., $Z = 10$, 25.4, 50.8, and

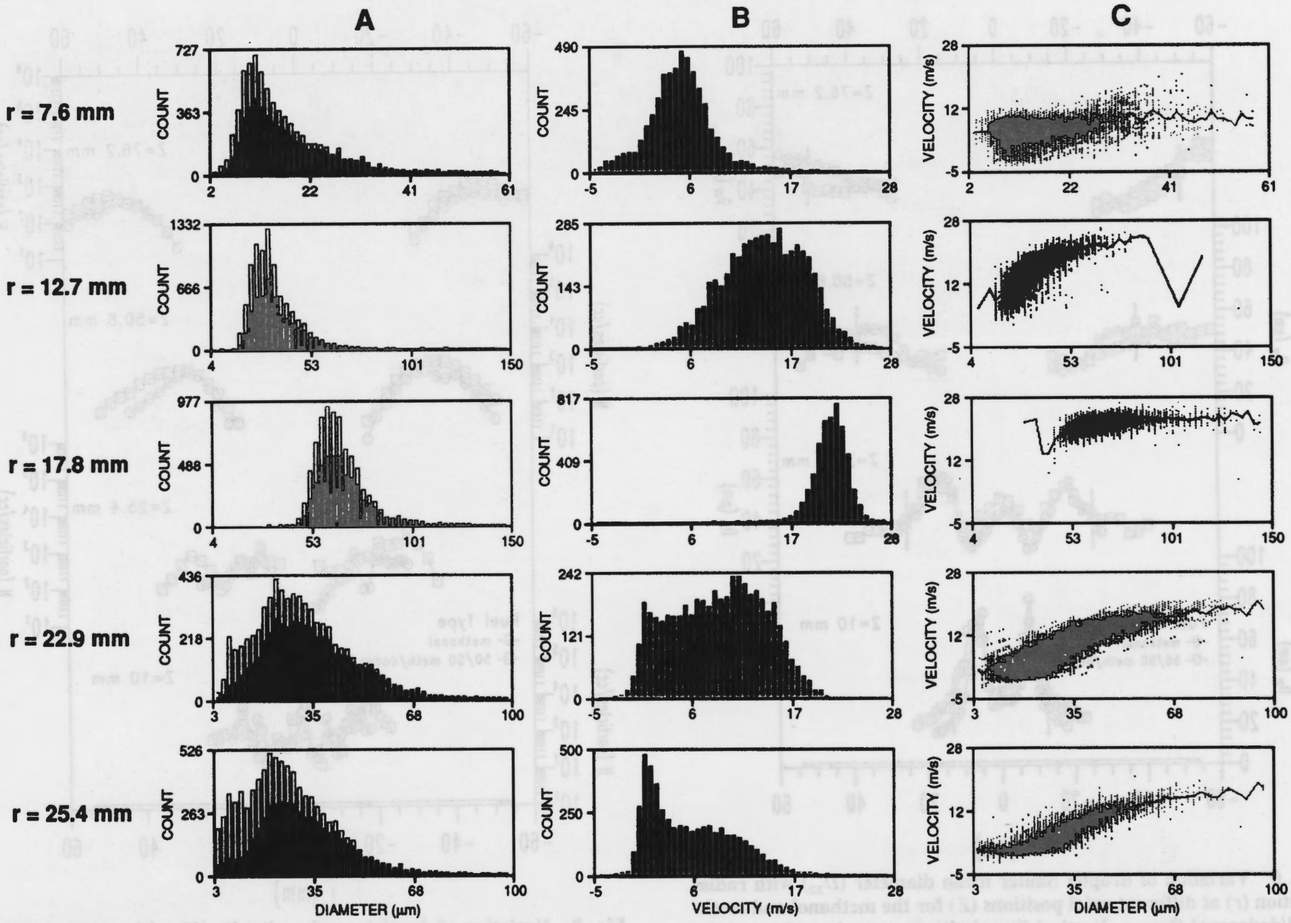

Fig. 9 Distribution of droplet a) size, b) velocity, and c) velocity/diameter correlations for the methanol flame at $Z = 25.4$ mm for different radial positions (r).

76.2 mm). Both of these results indicate that microexplosions may have occurred.

It is interesting to note that the total time to record 5000 validated data points for the mixture flame required less time than the methanol flame. The number of invalidated droplets (rejections) are generally lower for the methanol flame than for the mixture in regions where the number density is high (e.g., near the spray boundary). Several criteria are involved in invalidating droplet signals that include poor signal quality (low signal/noise ratio), multiple particles in the probe volume (coincidence), droplet asphericity (ligaments), reflections from droplets passing through the edge of the probe volume, and oblique droplet trajectories through the probe volume. In particular, droplet rejections may result from nonhomogeneities in the individual mixture droplets.

The occurrence of microexplosions for the mixture droplets is consistent with experiments performed at earth normal gravity on isolated moving droplets.[2] It is interesting that microexplosions of equivolume concentrations of methanol and dodecanol have not been observed in stationary free droplet combustion experiments performed in a buoyancy-free environment.[3] This fact may suggest the importance of liquid circulation within the droplet, which would be induced by buoyancy or by the movement of the droplet. The internal liquid circulation may distribute the mixture components within the droplet in a manner favorable to creating the necessary superheat conditions for microexplosions.

D. Size and Velocity Distributions

The size and velocity distributions of the individual droplets as they pass through the probe volume provide further insights for understanding the structure of the spray and microexplosions. A typical set of size and velocity distributions, and velocity/diameter correlations obtained for the methanol spray flame is presented in Fig. 9 at $Z = 25.4$ mm (a reference to indicate the position of the probe volume within the spray flame is provided in Fig. 4). The solid bars of the distribution represent the measured data on a flux (or temporal) basis, while the open bars represent the data corrected for variations in the effective measurement volume.[4] Also note the change in axes scales between distributions. In the methanol spray flame, the size and velocity distributions were monomodal within the spray boundary. As radial position increases from the centerline toward the spray boundary, a greater number of larger, higher velocity droplets were detected than smaller, lower velocity ones. This shift in the size and velocity distributions results in an increase in the mean properties. In addition, negative values of velocity indicate the presence of recirculated droplets in the probe volume near the spray centerline. The velocity/diameter correlations do not indicate any particular trend at radial positions between the spray centerline and boundary. However, in the region between the spray boundary and flame sheet (see $r = 22.9$ mm in Fig. 9) the correlation improves as droplet mean properties decrease. At positions between the outer spray boundary and flame sheet, bimodal velocity distributions were found. The lower velocity peak may be attributed to droplets entrained into the surrounding air flow field. The size and velocity distributions at other axial locations were found to be similar to that obtained at 10 mm.

The size and velocity distributions for the methanol/dodecanol flame are presented in Figs. 10 and 11 at $Z = 25.4$ and 50.8 mm, respectively. The results indicate similar trends to that of the methanol flame, except between the outer spray boundary and flame sheet where the velocity profiles were bimodal (e.g., see $Z = 50.8$ mm, $r = 33$ mm). At these positions the size distributions remain monomodal. There is, however, an increase in the number of smaller size droplets

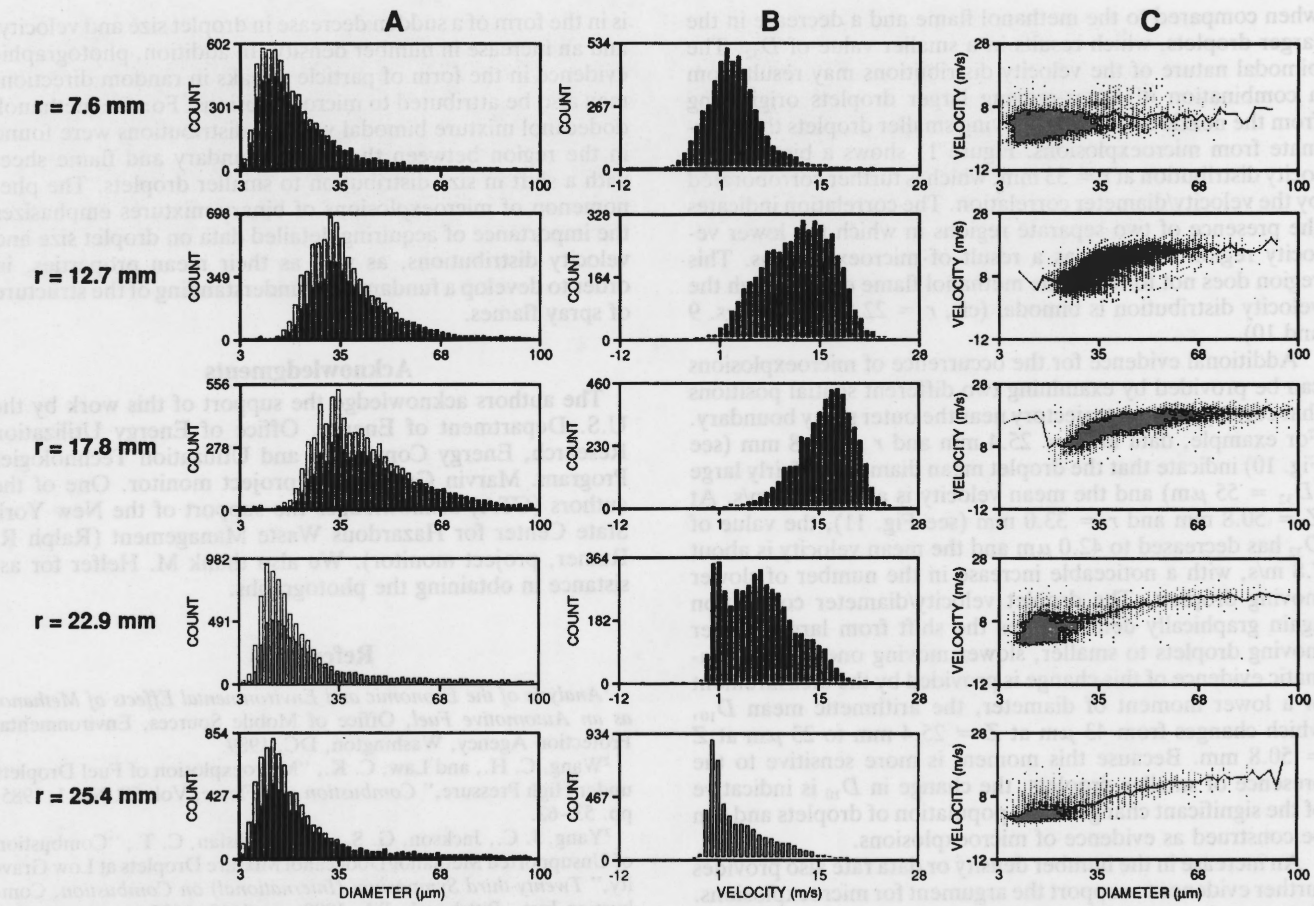

Fig. 10 Distribution of droplet a) size, b) velocity, and c) velocity/diameter correlations for the methanol/dodecanol flame at Z = 25.4 mm for different radial positions (r).

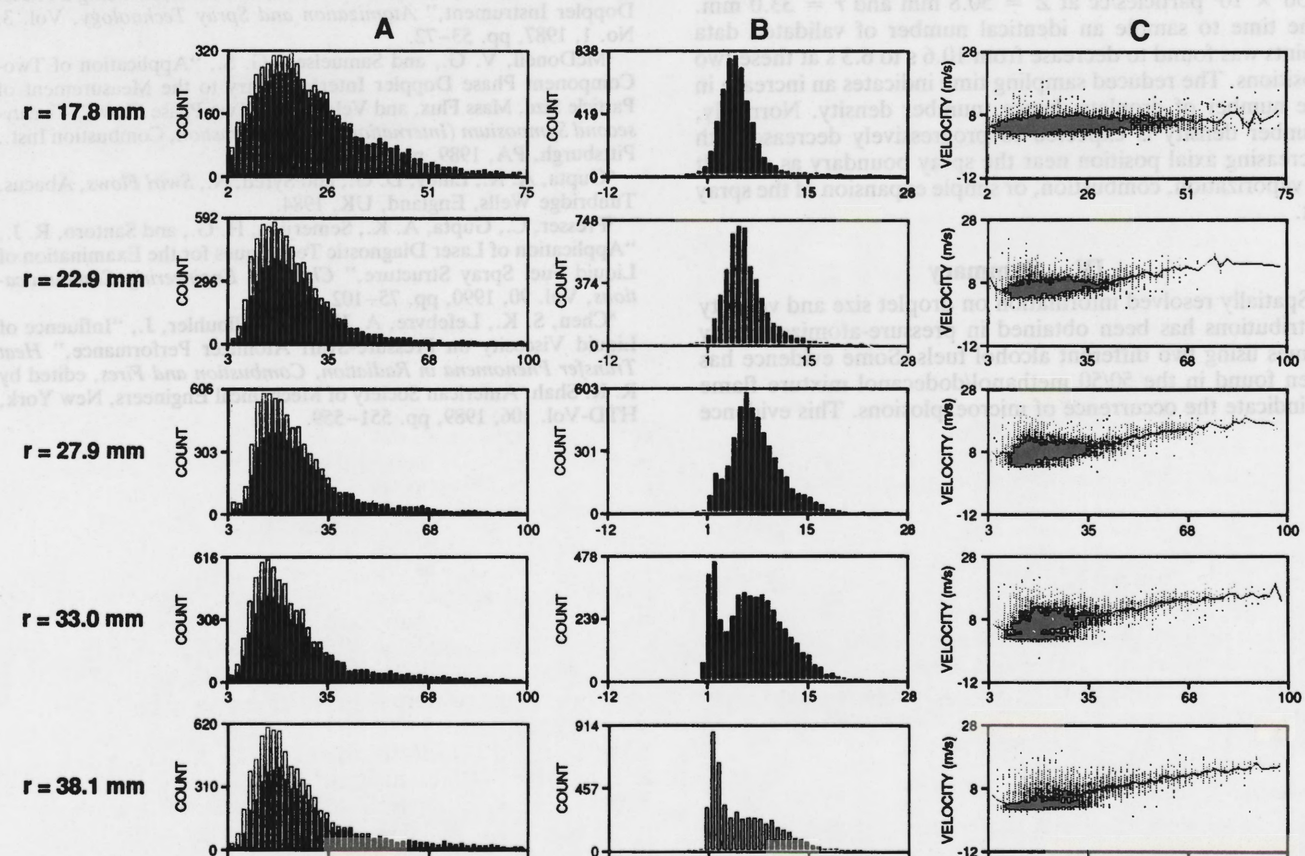

Fig. 11 Distribution of droplet a) size, b) velocity, and c) velocity/diameter correlations for the methanol/dodecanol flame at Z = 50.8 mm for different radial positions (r).

when compared to the methanol flame and a decrease in the larger droplets, which results in a smaller value of D_{32}. The bimodal nature of the velocity distributions may result from a combination of faster-moving larger droplets originating from the nozzle and slower-moving smaller droplets that originate from microexplosions. Figure 11 shows a bimodal velocity distribution at $r = 33$ mm, which is further corroborated by the velocity/diameter correlation. The correlation indicates the presence of two separate regions in which the lower velocity region develops as a result of microexplosions. This region does not form for the methanol flame even though the velocity distribution is bimodal (cf., $r = 22.9$ mm in Figs. 9 and 10).

Additional evidence for the occurrence of microexplosions can be provided by examining two different spatial positions that correspond to a trajectory near the outer spray boundary. For example, data at $Z = 25.4$ mm and $r = 17.8$ mm (see Fig. 10) indicate that the droplet mean diameter is fairly large ($D_{32} = 55$ μm) and the mean velocity is about 15.8 m/s. At $Z = 50.8$ mm and $r = 33.0$ mm (see Fig. 11), the value of D_{32} has decreased to 42.0 μm and the mean velocity is about 7.8 m/s, with a noticeable increase in the number of slower moving droplets. The droplet velocity/diameter correlation again graphically demonstrates the shift from larger, faster moving droplets to smaller, slower moving ones. More dramatic evidence of this change is provided by the measurement of a lower moment of diameter, the arithmetic mean D_{10}, which changes from 43 μm at $Z = 25.4$ mm to 23 μm at $Z = 50.8$ mm. Because this moment is more sensitive to the presence of smaller droplets, the change in D_{10} is indicative of the significant change in the population of droplets and can be construed as evidence of microexplosions.

An increase in the number density or data rate also provides further evidence to support the argument for microexplosions. For example, the number density was found to increase from 6.64×10^2 particles/cc at $Z = 25.4$ mm and $r = 17.8$ mm to 1.36×10^3 particles/cc at $Z = 50.8$ mm and $r = 33.0$ mm. The time to sample an identical number of validated data points was found to decrease from 10.6 s to 6.3 s at these two positions. The reduced sampling time indicates an increase in the number of droplets; hence, number density. Normally, number density is expected to progressively decrease with increasing axial position near the spray boundary as a result of vaporization, combustion, or simple expansion of the spray jet.

IV. Summary

Spatially resolved information on droplet size and velocity distributions has been obtained in pressure-atomized spray flames using two different alcohol fuels. Some evidence has been found in the 50/50 methanol/dodecanol mixture flame to indicate the occurrence of microexplosions. This evidence is in the form of a sudden decrease in droplet size and velocity, and an increase in number density. In addition, photographic evidence in the form of particle streaks in random directions may also be attributed to microexplosions. For the methanol/dodecanol mixture bimodal velocity distributions were found in the region between the spray boundary and flame sheet with a shift in size distribution to smaller droplets. The phenomenon of microexplosions of binary mixtures emphasizes the importance of acquiring detailed data on droplet size and velocity distributions, as well as their mean properties, in order to develop a fundamental understanding of the structure of spray flames.

Acknowledgments

The authors acknowledge the support of this work by the U.S. Department of Energy, Office of Energy Utilization Research, Energy Conversion and Utilization Technologies Program. Marvin Gunn is the project monitor. One of the authors (CTA) acknowledges the support of the New York State Center for Hazardous Waste Management (Ralph R. Rumer, project monitor). We also thank M. Helfer for assistance in obtaining the photographs.

References

[1]*Analysis of the Economic and Environmental Effects of Methanol as an Automotive Fuel*, Office of Mobile Sources, Environmental Protection Agency, Washington, DC, 1989.

[2]Wang, C. H., and Law, C. K., "Microexplosion of Fuel Droplets under High Pressure," *Combustion and Flame*, Vol. 59, No. 1, 1985, pp. 53–62.

[3]Yang, J. C., Jackson, G. S., and Avedisian, C. T., "Combustion of Unsupported Methanol/Dodecanol Mixture Droplets at Low Gravity," *Twenty-third Symposium (International) on Combustion*, Combustion Inst., Pittsburgh, PA, 1990, pp. 1619–1625.

[4]Bachalo, W. D., Houser, N. J., and Smith, J. N., "Behavior of Sprays Produced by Pressure Atomizers as Measured Using a Phase/Doppler Instrument," *Atomization and Spray Technology*, Vol. 3, No. 1, 1987, pp. 53–72.

[5]McDonell, V. G., and Samuelsen, G. S., "Application of Two-Component Phase Doppler Interferometry to the Measurement of Particle Size, Mass Flux, and Velocities in Two-Phase Flows," *Twenty-second Symposium (International) on Combustion*, Combustion Inst., Pittsburgh, PA, 1989, pp. 1961–1971.

[6]Gupta, A. K., Lilley, D. G., and Syred, N., *Swirl Flows*, Abacus, Tunbridge Wells, England, UK, 1984.

[7]Presser, C., Gupta, A. K., Semerjian, H. G., and Santoro, R. J., "Application of Laser Diagnostic Techniques for the Examination of Liquid Fuel Spray Structure," *Chemical Engineering Communications*, Vol. 90, 1990, pp. 75–102.

[8]Chen, S. K., Lefebvre, A. H., and Rollbuhler, J., "Influence of Liquid Viscosity on Pressure-Swirl Atomizer Performance," *Heat Transfer Phenomena in Radiation, Combustion and Fires*, edited by R. K. Shah, American Society of Mechanical Engineers, New York, HTD-Vol. 106, 1989, pp. 551–559.